Exchange interactions and Curie temperatures of Mn$_2$CoZ compounds

To cite this article: Markus Meinert *et al* 2011 *J. Phys.: Condens. Matter* **23** 116005

View the article online for updates and enhancements.

Related content

- Ab initio prediction of ferrimagnetism, exchange interactions and Curie temperatures inMn2TiZ Heusler compounds
  M Meinert, J-M Schmalhorst and G Reiss

- Search for half-metallic ferrimagnetism in V-based Heusler alloys Mn2VZ (Z = Al, Ga, In,Si, Ge, Sn)
  K Özdogan, I Galanakis, E aioglu et al.

- Ferrimagnetism and disorder of epitaxial Mn2xCoxVAl Heusler compound thin films
  Markus Meinert, Jan-Michael Schmalhorst, Günter Reiss et al.

Recent citations

- Magneto-electronic properties and tetragonal deformation of rare-earth-element-based quaternary Heusler half-metals: A first-principles prediction
  Xiaotian Wang *et al*

- Accelerated discovery of new magnets in the Heusler alloy family
  Stefano Sanvito *et al*

- Exchange interactions and Curie temperatures in Fe2 NiZ compounds
  Xiao-Ping Wei *et al*

Exchange interactions and Curie temperatures of Mn_2CoZ compounds

Markus Meinert, Jan-Michael Schmalhorst and Günter Reiss

Department of Physics, Thin Films and Physics of Nanostructures, Bielefeld University,
33501 Bielefeld, Germany

E-mail: meinert@physik.uni-bielefeld.de

Abstract
The generalized Heusler compounds Mn_2CoZ (Z = Al, Ga, In, Si, Ge, Sn, Sb) with the
Hg_2CuTi structure are of great interest due to their half-metallic ferrimagnetism. The complex
magnetic interactions between the constituents are studied by means of first principles
calculations of the Heisenberg exchange coupling parameters, and Curie temperatures are
calculated from those. Due to the direct Mn–Mn exchange interaction in Mn_2CoZ, the Curie
temperature decreases, although the total moment increases when the valence electron number
Z is increased. The exchange interactions are dominated by a strong direct exchange between
Co and its nearest neighbor Mn on the B site, which is nearly constant. The coupling between
the nearest neighbor Mn atoms scales with the magnetic moment of the Mn atom on the C site.
Calculations with different lattice parameters suggest a negative pressure dependence of the
Curie temperature, which follows from the decreasing magnetic moments. Curie temperatures
of more than 800 K are predicted for Mn_2CoAl (890 K), Mn_2CoGa (886 K), and Mn_2CoIn
(845 K).

(Some figures in this article are in colour only in the electronic version)

1. Introduction

Recently, the Mn_2YZ compounds with Hg_2CuTi structure have
attracted considerable theoretical and experimental activities,
where Y = Fe, Co, Ni, Cu [1–10]. Some of these compounds
have been characterized as half-metallic ferrimagnets. The
Hg_2CuTi structure is closely related to the structure of the
well-known Heusler compounds. The Mn_2YZ compounds
also follow the Slater–Pauling rule connecting the magnetic
moment m and the number of valence electrons N_V via $m =
N_V - 24$ in half-metallic Heusler compounds [11].

Half-metallic compounds are characterized by a gap for
either the spin-down or the spin-up density of states (DOS) at
the Fermi energy, so that an electric current has purely up or
down electrons. In applications that make use of spin polarized
currents, materials with this property are obviously favorable.
The concept was discovered by de Groot *et al* in band structure
calculations of the semi-Heusler compound NiMnSb [12].
Since then, many more systems were characterized as half-
metallic by band structure theory, in particular from the class
of Heusler compounds.

Heusler compounds have the general chemical formula
X_2YZ, where X and Y are transition metals, and Z is a
main group III, IV, or V element and adopt the $L2_1$ crystal
structure (space group $Fm\bar{3}m$). It can be imagined as four
interpenetrating fcc lattices with the basis vectors $A =
(0, 0, 0)$, $B = (1/4, 1/4, 1/4)$, $C = (1/2, 1/2, 1/2)$, and
$D = (3/4, 3/4, 3/4)$. The sites B and D are equivalent by
symmetry and occupied by the X element, whereas Y and Z
occupy the A and C sites. In the Hg_2CuTi structure, the B
and C sites are occupied by X, which makes them nearest
neighbors. This occupation is preferred with respect to the
Heusler structure if X has less valence electrons than Y [13, 7].
In this structure, the inversion symmetry is broken and it is
thus assigned to space group $F\bar{4}3m$. It can be thought of as a
generalization of the Heusler structure.

Half-metallic ferrimagnets have advantages over the well-
known half-metallic ferromagnets: due to the internal spin
compensation they have low magnetic moment and weak
stray field, while the Curie temperature can be high [14].
The probably best known half-metallic ferrimagnet among
the Heusler compounds is Mn_2VAl [15–19]. It has been
predicted to be a half-metallic ferrimagnet [20, 21] with a
low magnetic moment of 2 μ_B/formula unit (f.u.). The Curie
temperature of 760 K is the highest reported to date for the Mn_2

based (generalized) Heusler compounds and makes Mn_2VAl a promising compound for spintronics [17]. Apart from that, several other materials classes have been proposed to be half-metallic ferrimagnets [22, 23].

Ideally, an electrode material for spintronics would be a half-metal with tunable net moment. For net moment of zero, this would be a half-metallic antiferromagnet or fully compensated half-metallic ferrimagnet, and several materials have been predicted to show this unusual property [24–29]. However, half-metallic antiferromagnetism is limited to a small temperature range because of the inequivalent magnetic sublattices [30].

In the literature it has been noted that the Mn_2YZ compounds with Hg_2CuTi structure are dominated by direct exchange between the nearest neighbor Mn atoms, but direct calculations of the exchange interactions are missing. It is the scope of this paper to provide these calculations for the Mn_2CoZ compounds. We focus on this compound series because it has been experimentally synthesized, and band structure calculations suggested very large atomic moments and half-metallicity in most cases.

The half-metallicity of Mn_2CoZ is constituted by two processes [2]. First, a broad covalent gap of Mn(B) is created by covalent hybridization with Co and Mn(C), which form the (double tetrahedral) nearest neighbor shell. However, the final size of the minority gap is determined by the e_u–t_{1u} splitting in the hybridization of Co and Mn(C), which form each other's (octahedral) second nearest neighbor shells. Mn(B) states do not contribute to this hybridization because of the different symmetry transformations. Thus, the band gap is a d–d gap [31]. This situation is similar to the one in the Co_2MnZ Heusler compounds, where the e_u–t_{1u} splitting of the Co–Co hybridization governs the minority gap [11].

2. Computational approach

We performed our calculations with the spin polarized relativistic Korringa–Kohn–Rostoker package Munich SPRKKR [32]. The calculations were carried out in the full-potential mode with an angular momentum cutoff of $l_{max} = 3$ on a $28 \times 28 \times 28$ k point mesh (564 points in the irreducible wedge of the Brillouin zone). In order to further improve the charge convergence with respect to l_{max}, we employed Lloyd's formula for the determination of the Fermi energy [33, 34]. The exchange–correlation potential was modeled within the generalized gradient approximation of Perdew, Burke, and Ernzerhof [35] and the calculations were converged to about 0.1 meV. All calculations were carried out in the scalar-relativistic representation of the valence states, thus neglecting the spin–orbit coupling.

In the classical Heisenberg model the Hamiltonian of a spin system is given by

$$H = -\sum_{i,j} e_i e_j J_{ij}, \qquad (1)$$

with the Heisenberg pair exchange coupling parameters J_{ij}, and unit vectors e_i pointing in the direction of the magnetic moment on site i. SPRKKR allows to calculate the exchange

Table 1. Lattice parameters used for the calculations and resulting total and site resolved magnetic moments. The total magnetic moments are given in μ_B/f.u., the atomic magnetic moments are given in μ_B/atom.

Mn_2CoZ	a (Å)	m_{total}	m_{Co}	$m_{Mn(B)}$	$m_{Mn(C)}$	m_Z
Al	5.84	1.99	0.94	2.69	−1.59	−0.05
Ga	5.86	2.01	0.93	2.88	−1.78	−0.03
In	6.04[a]	1.95	0.99	3.16	−2.18	−0.02
Si	5.70	2.99	0.84	2.66	−0.50	−0.01
Ge	5.80	2.98	0.87	2.83	−0.72	0.01
Sn	5.96[a]	2.98	0.83	2.96	−0.81	−0.01
Sb	5.90	3.97	0.88	2.95	0.15	0.00

[a] Exp. lattice parameters: Mn_2CoIn 6.14 Å, Mn_2CoSn 6.06 Å.

coupling parameters by mapping the system onto a Heisenberg Hamiltonian. The parameters are determined within a real-space approach using the theory by Liechtenstein *et al* [36]. From the J_{ij} the Curie temperatures were calculated within the mean field approximation (MFA). For a single-lattice system the Curie temperature is given within the MFA by

$$\tfrac{3}{2}k_B T_C^{MFA} = J_0 = \sum_j J_{0j}. \qquad (2)$$

In a multi-sublattice system—as, e.g., the Heusler compounds with four sublattices—one has to solve the coupled equations

$$\tfrac{3}{2}k_B T_C^{MFA}\langle e^\mu \rangle = \sum_\nu J_0^{\mu\nu}\langle e^\nu \rangle, \qquad J_0^{\mu\nu} = \sum_{r \neq 0} J_{0r}^{\mu\nu}, \qquad (3)$$

where $\langle e^\nu \rangle$ is the average z component of the unit vector e_r^ν pointing in the direction of the magnetic moment at site (ν, r). The coupled equations can be rewritten as an eigenvalue problem:

$$(\Theta - TI)E = 0, \qquad \tfrac{3}{2}k_B\Theta_{\mu\nu} = J_0^{\mu\nu}, \qquad (4)$$

with a unit matrix I and the vector $E^\nu = \langle e^\nu \rangle$. The largest eigenvalue of the Θ matrix gives the Curie temperature [21, 37]. The r-summation in equation (3) was taken to a radius of $r_{max} = 3.0a$, where a is the lattice constant.

The lattice parameters were taken from Liu *et al* [2], who provide experimental values for Z = Al, Ga, In, Ge, Sn, Sb. For Mn_2CoSi we assumed the Mn_2CoGe parameter reduced by 0.1 Å, which is observed, e.g., for Co_2MnSi–Co_2MnGe [38]. The calculations of Mn_2CoIn and Mn_2CoSn were unstable at the experimental lattice parameters, but could be stabilized with slightly reduced values. All lattice parameters used here are summarized in table 1.

3. Results

3.1. Magnetic moments

The electronic structure calculations yield a half-metallic ground state in all cases with the exception of Mn_2CoGa and Mn_2CoIn. Our results for the total and site resolved magnetic moments are summarized in table 1. The total magnetic moments closely follow the Slater–Pauling rule for half-metallic Heusler compounds, so that we have magnetic

Table 2. Nearest and second nearest neighbor coordinations in Mn$_2$CoZ.

Distance (r/a)	0.433	0.50
Symmetry	T$_d$	O$_h$
Co	Mn(B)/Z	Mn(C)
Mn(B)	Mn(C)/Co	Z
Mn(C)	Mn(B)/Z	Co
Z	Mn(C)/Co	Mn(B)

moments of 2, 3, or 4 μ_B/f.u. if Z is a group III, IV or V element, respectively. Small deviations from the integer values arise from the angular momentum truncation at $l_{max} = 3$, which gives rise to a very small DOS in the minority gap. This is a typical observation when using the KKR method on ferromagnetic half-metals (see, e.g., Galanakis *et al* [11]). The magnetic moment of the Co atom is nearly constant for different Z materials, being about 0.9 μ_B. Similarly, the Mn(B) atom has a nearly constant magnetic moment in the range of 2.69–3.16 μ_B. In contrast, the moment of the Mn(C) atom changes considerably with the valence electron number and determines finally the total moment. All Mn$_2$CoZ compounds are ferrimagnetic due to the Mn(C) atom with the exception of Mn$_2$CoSb, which is a ferromagnet. In all cases the Z atom is nearly unpolarized. Only small changes are observed for the site resolved moments when Z is changed within one group. The increase of the absolute value of the Mn moments within one group can be traced to the lattice parameter change upon Z change. The orbital overlap is reduced with increasing lattice parameter, giving rise to weaker hybridizations (which is also the reason for the gap width reduction). Because of this reduction of itinerancy the quenching of the atomic moments is less effective and the moments become more atomic-like, i.e., larger.

Our results differ considerably from those given by Liu *et al* [2], who used the full-potential linearized augmented plane waves (FLAPW) method. The total magnetic moments are in very good agreement, but the atomic moments are smaller in our calculations by 0.3–0.7 μ_B for Mn(B) and Mn(C). In contrast, the magnetic moments of the Co atoms are nearly equal. Most notably, in our calculations Mn$_2$CoSb is ferromagnetic instead of ferrimagnetic. Therefore, we have checked our SPRKKR results with the FLAPW package Elk [39]. Our FLAPW results are concordant with the SPRKKR data, leaving the discrepancies with Liu *et al* unexplained.

Apart from these differences the DOS are in good agreement with [2] and all conclusions about the electronic structure given there are transferable to our calculations.

3.2. Exchange interactions and Curie temperatures

Figure 1 shows the Heisenberg exchange coupling parameters obtained from our calculations. To ease the following discussion, refer to table 2 for the atomic coordinations.

We start with the discussion of the Al–Ga–In series. It is notable that the exchange interactions are tightly confined to clusters of radius $r \leqslant a$. In particular, the inter-sublattice interactions have significant contributions only for

Table 3. Curie temperatures T_C^{MFA} calculated in the mean field approximation.

Mn$_2$CoZ	Al	Ga	In	Si	Ge	Sn	Sb
T_C^{MFA} (K)	890	886	845	578	579	536	567

the nearest and second nearest neighbors, while the intra-sublattice contributions are significant up to $r = a$. An exponential damping of the exchange interactions is expected for half-metals [40]; in the cases of Ga and In the damping is also present, but not as efficient as in the half-metallic case of Al. One observes clearly the dominating Co–Mn(B) and Mn(C)–Mn(B) nearest neighbor interactions, where the Mn(C)–Mn(B) interaction is clearly the stronger one. The Co–Mn(B) (second nearest neighbor interaction) is much weaker in comparison. In the graphs we omit the interactions with Z, because these are effectively zero for all distances. Co and Mn(C) couple antiferromagnetically to Mn(B), while Co and Mn(B) couple ferromagnetically. Hence, the antiparallel alignment of the Mn(C) moment is stable with respect to Mn(B) and Co. On the other hand, the intra-sublattice interactions are negative, which leads to a destabilization of the parallel alignment of the moments on one sublattice. It should be noted that in the Al–Ga–In series the Mn(C)–Mn(C) interaction is reduced on the first shell, while it is increased on the second shell at $r/a = 1$, where it becomes larger than the Co–Mn(C) inter-sublattice interaction.

For the Si–Ge–Sn series some differences to the previous results are notable. The most evident one is the much lower Mn(C)–Mn(C) interaction, but also the Co–Mn(B) interaction is significantly reduced. In particular, the Mn(C)–Mn(B) interaction is reduced by a factor of about 3, in very good agreement with the reduction of the Mn(B) moment. This indicates a strong direct exchange interaction, which is feasible because of the small Mn(B)–Mn(C) distance of typically 2.53 Å. It is remarkable that the Co–Mn(B) interactions are even slightly increased with respect to the Al–Ga–In series, although the site resolved magnetic moments are systematically lower. The additional loosely bound sp electron augments the direct exchange coupling here. Finally, the intra-sublattice interaction of Mn(B)–Mn(B) is found to be positive in all three compounds on the first shell, but the other intra-sublattice parameters are still negative.

Mn$_2$CoSb is special in this respect, since it is a ferromagnet with a small positive magnetic moment on the Mn(C) site. Accordingly, the Co–Mn(C) and Mn(C)–Mn(B) interactions are positive, and their values are in reasonable agreement with the reduction of the Mn(C) moment. In contrast, the Co–Mn(B) interaction is still large and is with the exception of Mn$_2$CoSi the largest one among all discussed compounds. The Mn(B)–Mn(B) interaction is negative again on the first and second shells. Such a periodicity with respect to the valence electron count of the system has been predicted by Şaşioğlu for some full Heusler compounds and occurs in the presence of indirect exchange interactions mediated by the conduction electrons [41].

From the exchange coupling parameters described above we calculated the Curie temperatures within the mean field
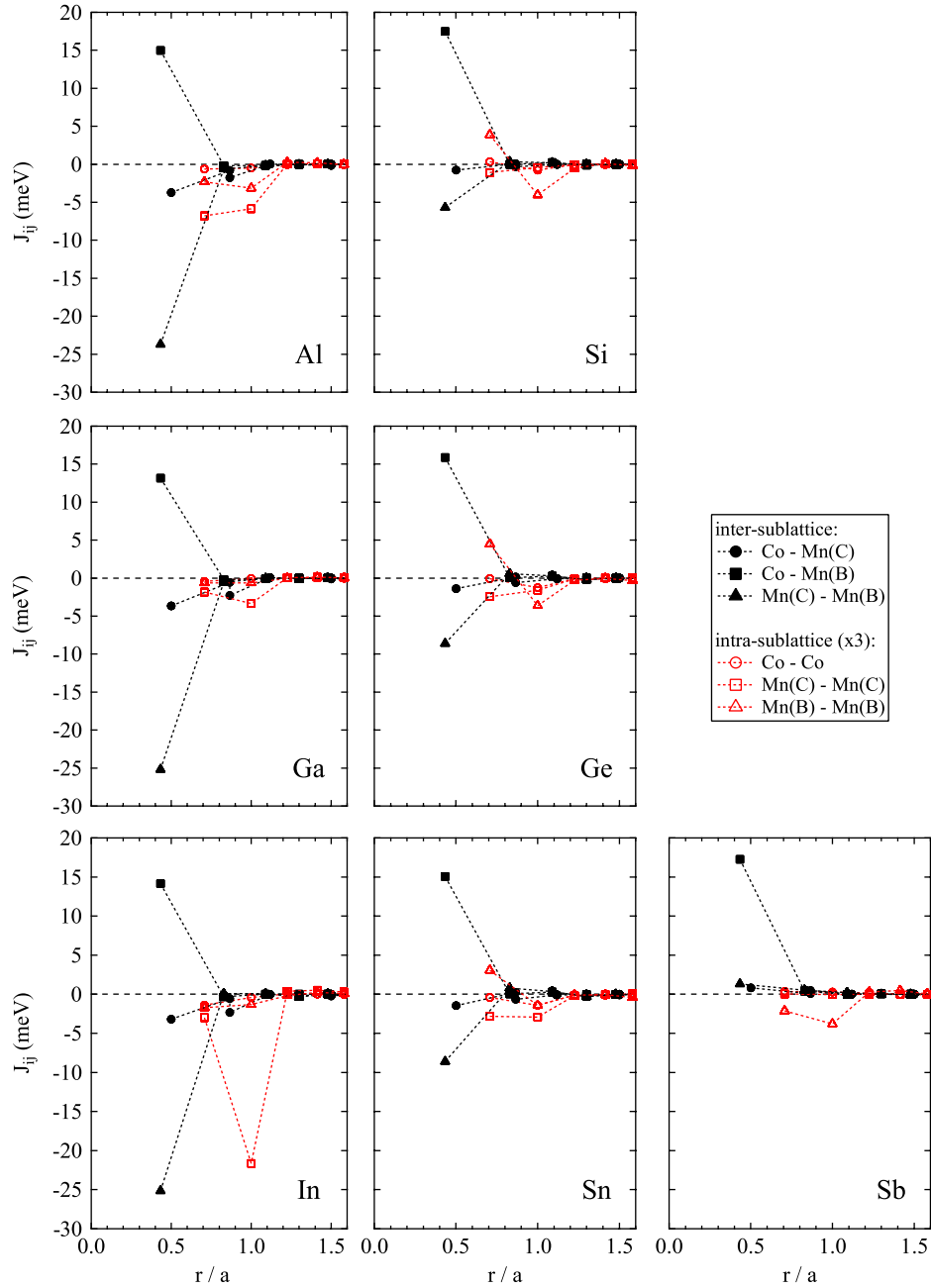
Figure 1. Heisenberg exchange coupling parameters J_{ij} for the Mn_2CoZ compounds as a function of the interatomic distance r. Note that the intra-sublattice interactions have been multiplied by three for clarity.

approximation (see table 3). The series Al–Ga–In has surprisingly high values of more than 800 K, even reaching almost 900 K for Mn_2CoAl. For the Si–Ge–Sn series we found moderate values between 500 and 600 K. The Curie temperature of Mn_2CoSb is similar as for the Si–Ge–Sn series. This is surprising at a first glance, because the Mn(C)–Mn(B) exchange interaction is so small here. It can be understood if we neglect all interactions but Mn(C)–Mn(B) and Co–Mn(B). In this case, $J_0^{\mu\nu}$ becomes a singular 3×3 matrix with two nonzero eigenvalues, which have the form of a root mean square of the Co–Mn(B) interaction and the Mn(C)–Mn(B) interaction. Obviously, if one interaction is significantly larger than the other (as, e.g., in Mn_2CoSn), then

the eigenvalues will be dominated by the larger interaction. This and the increased Co–Mn(B) exchange interaction explain the unexpected behavior.

However, what is most exciting about these results is the fact that Mn_2CoAl, Mn_2CoGa, and Mn_2CoIn have the highest Curie temperature among all ferrimagnetic intermetallic compounds reported to date. The Curie temperature decreases from one Z group to another, although the total moment increases. A behavior like this is unique for the Mn_2 based generalized Heusler compounds with Hg_2CuTi structure. The Co_2- and Mn_2-based genuine Heusler compounds show a scaling of the Curie temperature roughly proportional to the total moment upon change of the Z element [42, 43].

Nevertheless, the Mn₂CoZ compounds can be related to the Co₂-based Heusler compounds with the sum of the absolute values of the site resolved magnetic moments $\tilde{m}_{\text{total}}$: in, e.g., Mn₂CoAl we have $\tilde{m}_{\text{total}} = 5.27 \ \mu_\text{B}$, which is close the value of ferromagnetic Co₂MnSi (5 μ_B). The latter has a Curie temperature of 985 K [38], which is close to T_C^{MFA} of Mn₂CoAl. Further, the Curie temperature and $\tilde{m}_{\text{total}}$ are decreased with increasing Z electron number in Mn₂CoZ.

Naturally, the question about the accuracy of our Curie temperature calculation arises here. For the Mn₂CoZ series little data are available. Lakshmi *et al* reported T_C = 605 K for disordered Mn₂CoSn [4]. Dai *et al* reported 485 K for disordered Mn₂CoSb [5]. Hence, the T_C^{MFA} value underestimates the measured value in Mn₂CoSn and overestimates it for Mn₂CoSb, so no systematic trend can be stated here. It is *a priori* not clear which type of disorder can increase or decrease the Curie temperature, since the exchange interactions are highly site specific and quite complex. However, the calculated values reproduce the measured data within ±100 K. For comparison with Heusler compounds we also calculated the Curie temperatures of some compounds with available experimental data. The calculated (experimental) values are Co₂MnSi 1049 K (985 K) [38], Co₂TiSn 383 K (355 K) [44], Mn₂VAl 605 K (760 K) [17] and Mn₂VGa 560 K (783 K) [45]. We overestimate the correct values slightly in the two Co₂-based Heusler compounds, but the values for the two Mn₂-based compounds are underestimated by 25% or 150–200 K. It is not clear where this deviation stems from; two possible sources should be considered. On the one hand, the magnetic ground state itself could be incorrect. For example, correlation effects (via an LDA + U treatment) can significantly enhance the Curie temperature [46]. On the other hand, the calculation of the J_{ij} could be incorrect, due to the approximations made here. Liechtenstein's expression considers a long-wavelength approximation, thus it is less suited for materials with short-range magnetic order, which is important, e.g., in fcc Ni [47, 48].

In figure 2 we show the calculated Curie temperatures depending on the cluster radius taken into the summation in equation (3). As expected from the J_{ij} plots in figure 1, T_C^{MFA} is already determined by the nearest neighbor interactions in all compounds. Only weak changes are observed with increasing cluster radius and T_C^{MFA} is well converged at $r = 1.5a$. This plot helps us to identify the origin of the reduced Curie temperatures of Mn₂CoIn and Mn₂CoSn, which is apparently not the same. For Mn₂CoIn we can assign the jump at $r = a$ to the strong antiferromagnetic intra-sublattice interaction of Mn(C)–Mn(C). In Mn₂CoSn, the reduced ferromagnetic Mn(B)–Mn(B) intra-sublattice interaction on the third neighbor shell at $r = 0.707a$ is responsible for the reduction.

In order to shed some more light on the character of the exchange interactions and their dependence on the site specific magnetic moments, we calculated the ground states and exchange coupling parameters for Mn₂CoGe in the range of $a = 5.60$–5.95 Å. Thereby we can separate the influence of the Z valence electron count and the binding energy from
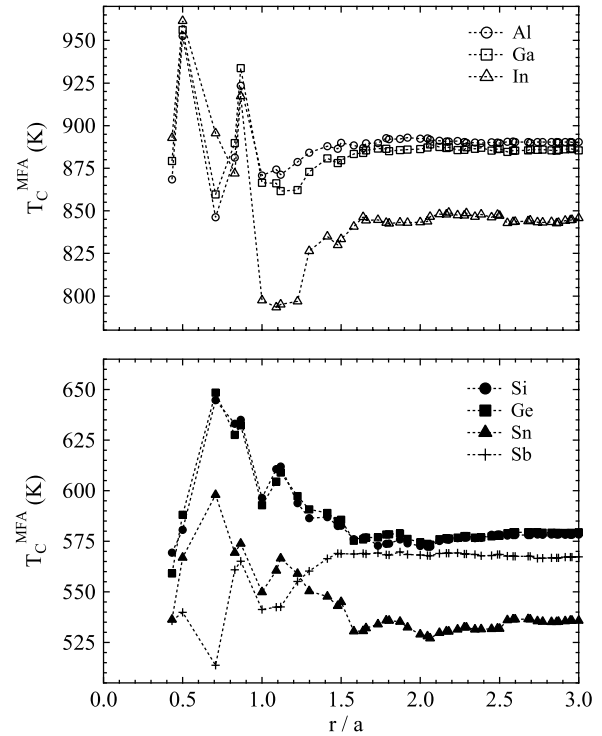

Figure 2. Curie temperature T_C^{MFA} as a function of the cluster radius.

geometric effects. The compound is a ferrimagnetic half-metal over the whole range, so we can expect minimal band structure effects on the calculations.

On the other hand, the site resolved magnetic moments change considerably with the lattice parameter (figure 3(a)). Their absolute values increase with increasing lattice parameter as already explained above. All moments vary approximately linearly such that the total moment remains at 3 μ_B/f.u. The moment of Mn(C) changes within the investigated range by more than a factor of three, from −0.34 to −1.12 μ_B. The compensation comes mostly from the Mn(B) site, and the Co moment remains fairly constant.

To display the exchange interactions in a compact form, we show the relevant contributions to the $J_0^{\mu\nu}$ matrix (equation (3)) in figure 3(b). The Co–Mn(B) interaction sum is nearly constant, although the magnetic moments increase. The nearest neighbor interaction remains nearly constant, but the weak longer-ranging interaction is significantly decreased and accounts for the decrease in the interaction sum. The constant nearest neighbor interaction is a result of two opposing processes, namely the increase of the moments and the reduction of exchange efficiency due to longer interatomic distances. In contrast, the interactions involving Mn(C) change considerably with the interatomic distance. The Mn(C)–Mn(B) exchange interactions increase by a factor of four, in agreement with the product $m_{\text{Mn(B)}} \cdot m_{\text{Mn(C)}}$. Further, the Co–Mn(C) interaction increases more than linearly with the lattice parameter, but the interaction is presumably indirect and no simple dependence is obvious. All these interactions lead to an increase of the Curie temperature with the lattice parameter. In contrast, the antiferromagnetic Mn(C)–Mn(C)
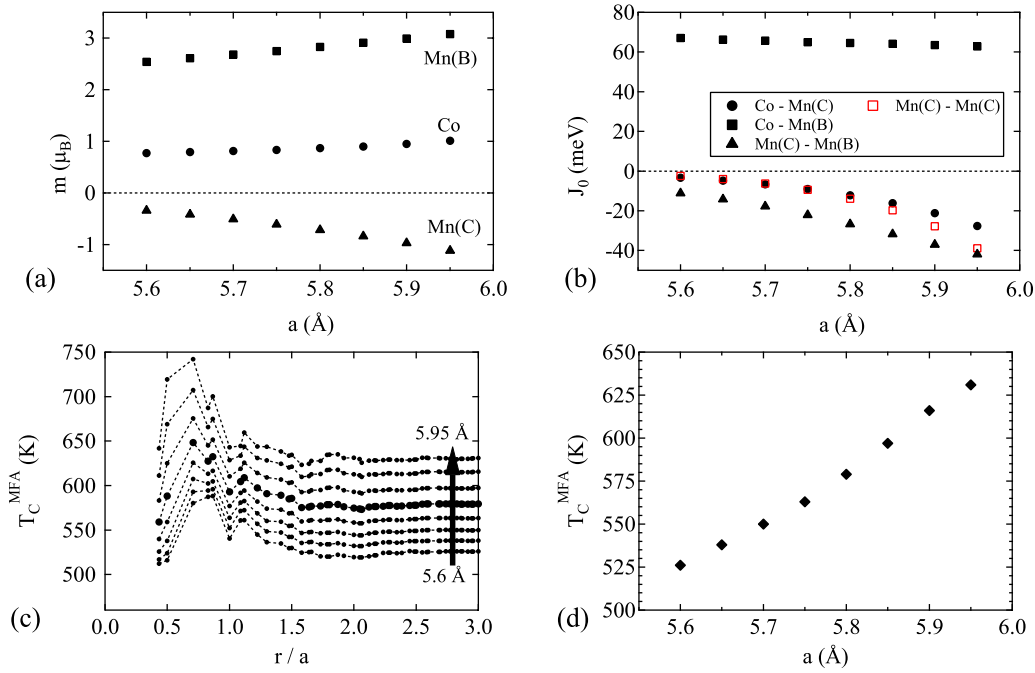
Figure 3. Lattice parameter dependences in Mn_2CoGe. (a) Site resolved magnetic moments. (b) $J_0^{\mu\nu}$ contributions. (c) Curie temperatures T_C^{MFA} depending on the cluster radius. (d) Curie temperatures T_C^{MFA}.

exchange interaction counteracts the ferrimagnetic order in the compound and reduces the Curie temperature. This influence is, however, negligible at small lattice parameter, but becomes quite large at the highest values, even compensating the Mn(C)–Mn(B) interaction. Notably, the Mn(C)–Mn(C) interaction is entirely governed by the nearest neighbor interaction and depends approximately on $m_{Mn(C)}^2$.

Figure 3(c) displays the Curie temperatures depending on the cluster radius. The general features of the exchange interactions are the same for all lattice parameters considered. However, there are some subtle differences on the second and third shells at $r = 0.5a$ and $r = 0.707a$, respectively. The change on the second shell can be traced back to the increased Co–Mn(C) interaction. Relative to the second shell, the contribution of the third shell is reduced. This arises from the increased antiferromagnetic Mn(C)–Mn(C) interaction discussed above. For clarity, figure 3(d) shows that the resulting Curie temperature T_C^{MFA} increases from 526 to 631 K with increasing lattice parameter.

In terms of a pressure dependence, the Curie temperature of Mn_2CoGe is thus predicted to decrease upon hydrostatic pressure, i.e., $dT_C/dp < 0$. This situation is very different from that in Heusler compounds, where usually $dT_C/dp > 0$ is found. However, it is in agreement with Castelliz's [49] and Kanomata's [50] empirical interaction curves. They propose a negative pressure coefficient of T_C for short Mn–Mn distances as in hexagonal MnAs or MnSb, but a positive coefficient at larger distances as in the Heusler compounds X_2MnZ. *Ab initio* calculations by Yamada *et al* on hexagonal MnAs [51] and by Şaşioğlu *et al* on the Heusler compound Ni_2MnSn [52] are in agreement with the experimentally observed pressure dependences. Recently, we have also calculated a positive pressure coefficient of T_C in the (hypothetical) Mn_2TiZ Heusler

compounds [43]. The Mn–Mn distance in the Mn_2CoZ compounds is even smaller than in the hexagonal MnAs or MnSb compounds, so a strong negative pressure dependence of T_C is in good agreement with the available experimental data.

Since the lattice parameter dependence of the Curie temperature is positive, the reduction of T_C^{MFA} in Mn_2CoIn and Mn_2CoSn (which have the largest lattice parameters within their groups) can be ascribed to a binding energy effect due to the high-lying valence states in In and Sn.

4. Conclusion

We have performed *ab initio* band structure calculations with the full-potential Korringa–Kohn–Rostoker method on the Mn_2CoZ compounds with Hg_2CuTi structure. The exchange interaction parameters obtained from the calculations are found to be governed by the Co–Mn(C) exchange, which is of direct nature. When Z = Al, Ga, In, the Mn(C)–Mn(C) interaction is the dominating one, which is direct as well. The indirect, long-ranged interactions are exponentially damped and thus weak, and the intra-sublattice interactions are mostly antiferromagnetic. Curie temperatures calculated within the mean field approximation are in reasonable agreement with experimental data for Mn_2CoSn and Mn_2CoSb. The Curie temperatures show an anomalous dependence on the total moment, which is different from the full Heusler compounds. For Mn_2CoAl we predict an exceptionally high Curie temperature of 890 K, although the total moment of the compound is only 2 μ_B/f.u. The dependence of the exchange parameters on the lattice parameter in Mn_2CoGe suggests a negative pressure dependence of T_C in the Mn_2CoZ compounds, which originates from the exchange interactions of Mn(C)–Mn(B) and Co–Mn(C).

Acknowledgments

References

[1] Luo H Z, Zhang H W, Zhu Z Y, Ma L, Xu S F, Wu G H, Zhu X X, Jiang C B and Xu H B 2008 *J. Appl. Phys.* **103** 083908
[2] Liu G D, Dai X F, Chen J L, Li Y X, Xiao G and Wu G H 2008 *Phys. Rev.* B **77** 014424
[3] Xing N, Li H, Dong J, Long R and Zhang C 2008 *Comput. Mater. Sci.* **42** 600
[4] Lakshmi N, Sharma R K and Venugopalan K 2005 *Hyperfine Interact.* **160** 227
[5] Dai X, Liu G, Chen L, Chen J and Wu G 2006 *Solid State Commun.* **140** 533
[6] Helmholdt R B and Buschow K H J 1987 *J. Less-Common Met.* **128** 167
[7] Luo H, Liu G, Feng Z, Li Y, Ma L, Wu G, Zhu X, Jiang C and Xu H 2009 *J. Magn. Magn. Mater.* **321** 4063
[8] Luo H, Meng F, Feng Z, Li Y, Zhu W, Wu G, Zhu X, Jiang C and Xu H 2009 *J. Appl. Phys.* **105** 103903
[9] Wei X P, Hu X R, Mao G Y, Chu S B, Lei T, Hu L B and Deng J B 2010 *J. Magn. Magn. Mater.* **322** 3204
[10] Li S T, Ren Z, Zhang X H and Cao C M 2009 *Physica* B **404** 1965
[11] Galanakis I, Dederichs P H and Papanikolaou N 2002 *Phys. Rev.* B **66** 174429
[12] de Groot R A, Mueller F M, van Engen P G and Buschow K H J 1983 *Phys. Rev. Lett.* **50** 2024
[13] Luo H, Zhu Z, Ma L, Xu S, Zhu X, Jiang C, Xu H and Wu G 2008 *J. Phys. D: Appl. Phys.* **41** 055010
[14] Pickett W E and Moodera J S 2001 *Phys. Today* **54** 39
[15] Itoh H, Nakamichi T, Yamaguchi Y and Kazama N 1983 *Trans. Japan Inst. Met.* **24** 265
[16] Yoshida Y, Kawakami M and Nakamichi T 1981 *J. Phys. Soc. Japan* **50** 2203
[17] Jiang C, Venkatesan M and Coey J M D 2001 *Solid State Commun.* **118** 513
[18] Ishida S, Asano S and Ishida J 1984 *J. Phys. Soc. Japan* **53** 2718
[19] Weht R and Pickett W E 1999 *Phys. Rev.* B **60** 13006
[20] Özdoğan K, Galanakis I, Şaşioğlu E and Aktaş B 2006 *J. Phys.: Condens. Matter* **18** 2905
[21] Şaşioğlu E, Sandratskii L M and Bruno P 2005 *J. Phys.: Condens. Matter* **17** 995
[22] Nakamura K, Ito T and Freeman A J 2005 *Phys. Rev.* B **72** 064449
[23] Galanakis I, Özdoğan K, Şaşioğlu E and Aktaş B 2006 *Phys. Rev.* B **74** 140408
[24] van Leuken H and de Groot R A 1995 *Phys. Rev. Lett.* **74** 1171
[25] Pickett W E 1998 *Phys. Rev.* B **57** 10613
[26] Akai H and Ogura M 2006 *Phys. Rev. Lett.* **97** 026401
[27] Galanakis I, Özdoğan K, Şaşioğlu E and Aktaş B 2007 *Phys. Rev.* B **75** 172405
[28] Özdoğan K and Galanakis I 2009 *J. Magn. Magn. Mater.* **321** L34
[29] Galanakis I, Özdoğan K, Şaşioğlu E and Aktaş B 2007 *Phys. Rev.* B **75** 092407
[30] Şaşioğlu E 2009 *Phys. Rev.* B **79** 100406
[31] Fang C M, de Wijs G A and de Groot R A 2002 *J. Appl. Phys.* **91** 8340
[32] Ebert H *et al* 2009 *The Munich SPR-KKR Package, Version 5.4* http://olymp.cup.uni-muenchen.de/ak/ebert/SPRKKR
Ebert H 2000 Fully relativistic band structure calculations for magnetic solids: formalism and application *Electronic Structure and Physical Properties of Solids* (*Lecture Notes in Physics* vol 535) ed H Dreyss (Berlin: Springer) p 191
[33] Lloyd P and Smith P V 1972 *Adv. Phys.* **21** 69
[34] Zeller R 2008 *J. Phys.: Condens. Matter* **20** 035220
[35] Perdew J P, Burke K and Ernzerhof M 1996 *Phys. Rev. Lett.* **77** 3865
[36] Liechtenstein A I, Katsnelson M I, Antropov V P and Gubanov V A 1987 *J. Magn. Magn. Mater.* **67** 65
[37] Anderson P W 1963 Theory of magnetic exchange interactions: exchange in insulators and semiconductors *Solid State Physics* vol 14, ed F Seitz and D Turnbull (New York: Academic) pp 99–214
[38] Webster P J 1971 *J. Phys. Chem. Solids* **32** 1221
[39] *Elk Version 1.1.4* http://elk.sourceforge.net
[40] Rusz J, Bergqvist L, Kudrnovský J and Turek I 2006 *Phys. Rev.* B **73** 214412
[41] Şaşioğlu E, Sandratskii L M and Bruno P 2008 *Phys. Rev.* B **77** 064417
[42] Kübler J, Fecher G H and Felser C 2007 *Phys. Rev.* B **76** 024414
[43] Meinert M, Schmalhorst J M and Reiss G 2011 *J. Phys.: Condens. Matter* **23** 036001
[44] Majumdar S, Chattopadhyay M K, Sharma V K, Sokhey K J S, Roy S B and Chaddah P 2005 *Phys. Rev.* B **72** 012417
[45] Kumar K R, Kumar N H, Markandeyulu G, Chelvane J A, Neu V and Babu P D 2008 *J. Magn. Magn. Mater.* **320** 2737
[46] Thoene J, Chadov S, Fecher G, Felser C and Kübler J 2009 *J. Phys. D: Appl. Phys.* **42** 084013
[47] Antropov V P 2003 *J. Magn. Magn. Mater.* **262** L192
[48] Antropov V P 2006 *J. Magn. Magn. Mater.* **300** e574
[49] Castelliz L 1955 *Z. Metall.* **46** 198
[50] Kanomata T, Shirakawa K and Kaneko T 1987 *J. Magn. Magn. Mater.* **65** 76
[51] Yamada H, Terao K, Kondo K and Goto T 2002 *J. Phys.: Condens. Matter* **2002** 11785
[52] Şaşioğlu E, Sandratskii L M and Bruno P 2005 *Phys. Rev.* B **71** 214412